Journal of Nanotechnology & Advanced Materials
An International Journal

H_2 Sensing Characterization of Pd-Doped CuO Nanoparticles; Synthesized by Solvothermal method

S. J. Musevi[1], A. Aslani[2, 3]* and H. Salimi[4]

[1]*Department of Chemistry, Shahid Beheshti Technical Faculty, Technical and Vocational University, Iran.*
[2]*Department of Nanobiotechnology Research Center, Baqiyatallah University Medical of Science, Iran.*
[3]*Department of Basic Science, Jundi Shapur University of Technology, Dizful, Islamic Republic of Iran*
[4]*Textile Engineering Department, Amir-Kabir University of Technology, Tehran, Islamic Republic of Iran.*

Email: Erkin_Musevi@hotmail.com[1], *a.aslani110@yahoo.com, aslani@jsu.ac.ir*[2], *nanochemistry@yahoo.com*[3]
Received: 8 Feb. 2012; Revised 15 May. 2012; Accepted 23 Jul. 2012

Abstract: Semiconductor oxides are important materials in gas-detection systems and can be improved by enhancing the sensitivity and selectivity of oxide sensors to specific gases. This research investigates the effect of palladium dopant (Pd) on the hydrogen gas-sensing ability of CuO nanoparticles. Photolithography was used to pattern electrodes on various concentrations of Pd-doped CuO thin films deposited on silicon oxide substrate, and these devices were subsequently used to measure the electrical resistance in response to hydrogen gas flow. Both nanoparticles and gas-sensing characterization were conducted on the CuO thin-film samples. For the nanoparticles characterization of the thin films, scanning electron microscopy (SEM) was used to determine the effect of various concentrations of dopant on the grain structure. X-Ray Photoelectron Spectroscopy (XPS) was used to verify the composition of the Pd-doped CuO thin films; X-Ray Diffraction (XRD) was used to determine the crystal structure of the doped thin films. For the gas-sensing characterization, the three key assessments used to characterize the sensitivity of CuO thin films were comparisons between CuO thin-film sensors and a commercial sensor, comparisons between CuO thin-film sensors and the exposure of the CuO thin films to UV light.

Keywords: gas sensing, CuO, nanoparticles, H2, solvothermal

Introduction:

Nanostructured metal oxides have been the subject of great attention in the field of nanotechnology both from a fundamental and industrial point of view. For example, their peculiar electrical properties make them suitable as active sensing materials in resistive sensors, with enhanced performance with respect to bulk materials [1]. The ability to control the particle size of metal oxide nanoparticles is of crucial importance in this respect [2–6]. Great attention is also addressed to the particle morphology and shape [2]. Various shapes can exhibit completely different physical properties and performances; therefore it is often highly desirable to have pure materials with controlled morphology. However, controlling the morphology of materials is not simple as controlling their particle size, yet. As a matter of fact, there is considerable interest in developing novel methods for the preparation of metal oxide nanoparticles possessing particular morphological properties and shape, for potential applications in gas sensing [7–9]. Moreover, for practical applications, the main challenge consists in finding cost-effective and scalable synthesis methods for the production of these nanostructures. On the basis of these considerations, syntheses of metal oxide nanostructures by chemical processes are more suited compared to physical ones. Due to the well-known surface conductivity of CuO, a great deal of attention has been given to this material for gas sensors applications. In order to enhance the sensing properties of copper oxide-based resistive gas sensors, suitable CuO nanostructures with controlled size are preferred [10–15]. Both theoretical and experimental works have been carried out in order to elucidate the relation between the sensitivity and the microstructure of CuO elements for gas sensors. Moreover, many researches found that the sensor based on sol–gel processed nanopowders is more sensitive to CO than that based on nanotetrapods. To rationalize the behavior of metal oxide nanostructures, Yamazoe et al. developed a new general model on the roles of shape and size of crystals in semiconductor resistive gas sensors on the basis of electron-depleted conditions [16, 17]. The model proposed confirms that the gas sensitivity increases with decreasing the

crystal size as it was experimentally proven for many cases, and predicts that crystals in spherical shape would show higher sensitivity than those in columnar shape. However, the effect of the nanostructure on the sensing properties in metal oxide-based resistive gas sensors is not yet fully understood and requires further investigations.

On the other hand, in recent years, coppric oxide (CuO) has been received extensive investigations for its prospective applications in many fields. CuO is a p-type semiconductor with a narrowband gap of 1.4 eV [18]. It has similar properties with high-Tc super-conducting cuprates but consists of Cu–O bonding only, so it has been used as a basic material in high-Tc superconductors [19, 20]. It also can be used potentially in gas sensors, solar cells, FE emitters, electronic cathode materials and catalysts in organic reactions [21–25]. Many methods have been developed to prepare CuO with various morphologies. Li et al. synthesized nano-dendrite like CuO via hydrothermal route [26].

A gas sensor is a device that is used to detect the presence or amount of a particular gas. Metal oxides have been undergoing extensive research due to their gas-sensing capabilities and have been applied in the automotive and aerospace industries for the detection of exhaust gases for environmental protection; the domestic sector in fire alarms and carbon monoxide sensors; the medical field for patient monitoring and diagnostics; and security and defense departments for tracing explosives and toxic gases [27]. One of the most critical needs in gas sensing is to develop hydrogen sensors for detection in biological functions and in fuel cells that are able to selectively detect hydrogen gas near room temperature and that are relatively inexpensive and portable [28, 29]. CuO, an oxide semiconductor, is an important prospect for hydrogen gas sensing because it is bio-safe and its nanostructures are simple to fabricate. Four main factors that affect its hydrogen-sensing ability still need to be studied and optimized: sensitivity, selectivity, stability, and response and recovery time [30]. Sensitivity the ability to detect minute quantities of a gas affects the performance of a gas sensor [31]. A large surface-to-volume ratio corresponds to a higher sensitivity, which has led to an interest in oxide nanostructures, which have ultrahigh surface-to-volume ratio [27]. Another very important property of a gas sensor is selectivity being able to distinguish a particular gas from all others. Oxides cannot easily distinguish between different types of gases, but adding certain dopants to them increases their selectivity. Another problem with oxide sensors is that they require high operating temperatures, which degrade the material and reduce the stability of the nanostructure sensors. The response and recovery time, or the time taken for the sensor to reach 90% of its saturation after applying or switching off the particular gas, is another important factor in the performance of a gas sensor [31]. The primary goal of this research is to study the effect of varying the concentration of Pd dopant in CuO thin-film nanostructure devices in order to optimize the devices performance during exposure to hydrogen gas.

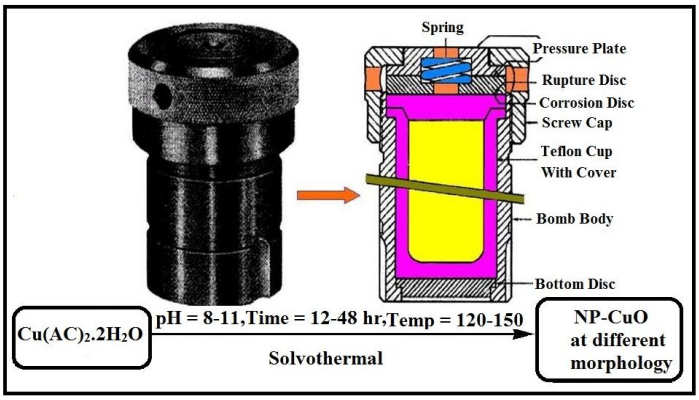

Scheme 1. The schematic formation of CuO nanostructures by solvothermal method without any additives.

Gas-sensor devices operate by converting chemical information from a chemical reaction with the gas molecule to an analytical signal [31]. CuO gas-sensor mechanisms involve the adsorption of oxygen on the oxide surface and create a charge transfer between the adsorbed oxygen and the target gas molecules,

which leads to a change in surface resistance of the sensor device [29, 32]. When a CuO sensor is exposed to air, an oxygen molecule adsorbs on the surface of the material and forms an O2- ion that creates a high resistance state in air and a high sensitivity [27]. This is the reason CuO gas-sensor devices have been fabricated as single crystals, thin films, nanoparticles, and various other nanostructures with small grain sizes. The adsorption reaction may occur due to a very high surface area-to-volume ratio, allowing for higher sensitivity in gas sensing [27, 29, and 31]. In addition to CuO nanoparticles for higher sensitivity, CuO is often doped with different materials to create catalytically active sites on the surface of the hydrogen gas sensor. This increases the dissociation of hydrogen to its more reactive form, increasing the selectivity of the gas-sensor device to hydrogen gas [30, 31]. Specifically, the selectivity for detecting hydrogen with CuO nanoparticles was greatly magnified by the doping of Pd onto the surface of the nanoparticles [28]. The addition of Pd to CuO thin films resulted in a reduction of conductance due to an increase in oxygen absorption, which increased the sensitivity from 60% for CuO to 99.8% in the doped CuO [32]. One of the main problems with commercial sensors is that they operate at high temperatures, which degrades the material and also decreases the stability and recoverability of these devices. Doping CuO with Pd has been shown to increase the stability of the nanoparticles and thin-film sensor devices and has also improved the response and recovery time of these devices to hydrogen gas [29]. The reason that Pd particles enhance the gas-sensing ability of oxides is that when Pd particles are exposed to hydrogen, they adsorb the gas and swell slightly to form palladium hydride. The different oxide gas sensors rely on the different conductivity of palladium and palladium hydride to indicate hydrogen concentration [33]. This study was aimed at comparing the doping effects of Pd on CuO nanoparticles thin-film sensors as well as optimizing the concentration of Pd in order to enhance the performance of these different gas-sensor devices to hydrogen gas in terms of the sensitivity, selectivity, stability, and response and recovery time.

Experimental:

The reaction of Cu acetate at different conditions of pH to form CuO nanoparticles has been shown in scheme 1. In a typical procedure, 2 mmol of Cu(Ac) 2.2H2O was added into 20 ml of EtOH/CH2Cl2. The mixture was stirred vigorously for 30 min and desired pH is reached (Table1) under vigorous agitation then mixture sealed in a Teflon-lined stainless-steel autoclave. The tank was heated and maintained at 120-190 ℃ for 12, 24, 36 and 48 hr, and then allowed to cool down to -10 ℃ temperature rapidly. The product was collected by centrifugation and washed with acetone and ethanol several times to remove the excessive reactants and by products. (Table 1). Then it was calcinated under vacuum at 600 °C for 2 hr. The resulting powder was collected for further characterization. X-ray powder diffraction (XRD) measurements were performed using a Philips diffractometer of X'pert Company with mono chromatized Cukα radiation. The particle sizes of selected samples were estimated using the Sherrer method. The samples were characterized by a scanning electron microscope (SEM) (Philips XL 30) with gold coating. The luminescent properties were investigated using an F-4500 FL spectrophotometer.

On the other hand to study the effect of Pd dopant on CuO thin-film gas sensor devices, different sol-gels for the silicon substrate were prepared using 0%, 1%, 2%, 4%, and 8% of Pd and 1.0 M CuO. These doped 1.0 M CuO sol-gels were then spin-coated onto silicon oxide substrate three times and annealed at 600 ℃ for 2 hr to create thin-film nanoparticles. SEM images were taken of the annealed samples at 50, 60, 80, and 100 K magnification settings in order to determine the effects of the different concentrations of Pd on the grain structure of CuO thin film. SEM images were also taken of the cross-section of the CuO thin film to determine the thickness of the film. SEM images were also taken of the CuO nanoparticles. EDAX was conducted using the SEM to confirm the presence of Cu, O, and Pd on the CuO thin-film samples; XPS was used as a more sensitive measure than EDAX to determine the presence of these elements. XRD was then used to determine the crystal structure of the annealed CuO thin films [34-36].

The second major analysis of the hydrogen sensing characteristics of CuO thin film compared the CuO thin film. Both samples were analyzed at room temperature with UV light exposure and three cycles of 100 sccm (2.5%) hydrogen gas flows. Although this research involved mostly the analysis of CuO nanoparticles, the third analysis involved the same conditions as the previous analysis but compared the

CuO thin film and the CuO nanoparticles to determine which dimensional structure had a better sensitivity in response to hydrogen gas flow.

Result and Discussion:

Nanostructure Characterization:

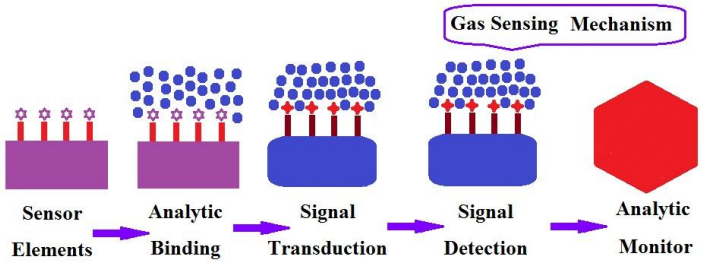

Fig. 1: the schematic gas-sensing mechanism can be explained by five processes

The reaction of Cu acetate at different conditions of pH to form CuO nanoparticles has been shown in scheme 1. In Figure 1 the schematic gas-sensing mechanism can be explained by five processes. (1) Sensor elements consist of the different type of structures of the gas-sensing material. (2) Analytic binding involves the binding of target gas molecules onto the surface of the sensor elements. (3) Signal transduction involves a surface reaction occurring between the target gas molecules and the surface of the sensor elements, which consists primarily of oxidation-reduction reactions between the oxygen on the surface and the target gas molecule. (4) The chemical reaction on the surface is interpreted by a change in resistance of the gas-sensor device. (5) The observed change in resistance is then recorded and analyzed.

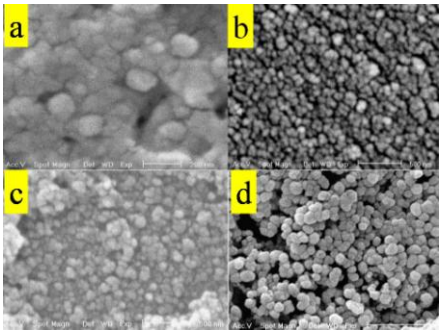

Fig. 2 Typical SEM micrographs of the samples (a) CuO-1 (b) CuO-2 (c) CuO-3 and (d) CuO-4 with distinct morphologies.

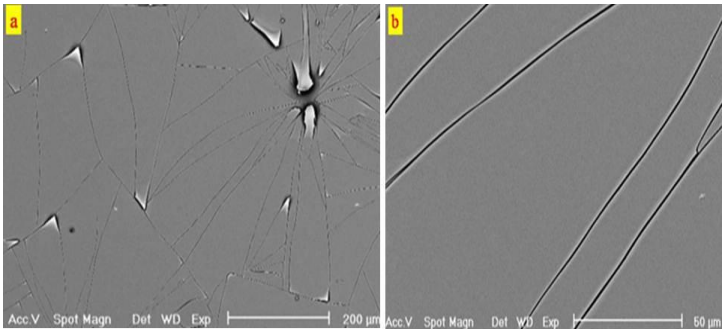

Fig. 3. The cross-section of the thin film shows that the thickness of the CuO thin films.

In Figure 2 (a, b, c and d), the SEM micrographs of four typical samples with distinct morphologies are presented. All the SEM images of the annealed Pd-doped CuO thin-film samples were taken at 80 k magnification (a) 0% Pd-CuO (b) 1% Pd-CuO (c) 2% Pd-CuO (d) 8% Pd-CuO. While the Figures shows the formation of CuO nanoparticles of about 70 nm average size, while all these structures were synthesized almost at the same reaction temperature and time with EtOH/CH2Cl2 contents, the reactant content in the reaction mixture was different. It is important to mention that the structures were well reproducible when the growth parameters were kept unchanged. However, the size of the nanoparticles could be varied to some extent by varying the reaction time. In Figure 3 (a and b) the cross-section of the thin film shows that the thickness of the CuO thin film is about 20 nm. The SEM image of the CuO Nano film shows a structure with less porosity and smaller grain sizes than the CuO nanoparticles. In Figure 4, the XRD spectra of the nanostructures synthesized are presented. All the XRD peaks were indexed in Figure 4, and they agreed well with the standard CuO of hexagonal structure. The results of XRD powder

patterns indicated that the experimental data are in good agreement with the simulated XRD powder patterns based on the reference data. Hence these compounds obtained as a mono-phase. The broadening of the peaks indicated that the particles were of nanometer scale. Estimated from the sherrer formula, $D = 0.891\lambda/\beta\cos\theta$, where, D is the average grain size, λ is the X-ray wavelength (0.15405 nm), and θ and β are the diffraction angle and full-width at half maximum of an observed peak, respectively. Figure 5 show the XPS Spectrum of 12% Pd-CuO thin film indicating primarily the presence of Cu, O, Pd, and Si.

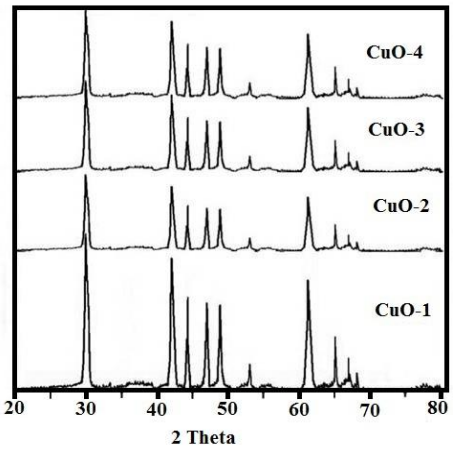

Fig. 4. XRD patterns of the CuO nanostructures grown with different pHs. See samples details in Table 1.

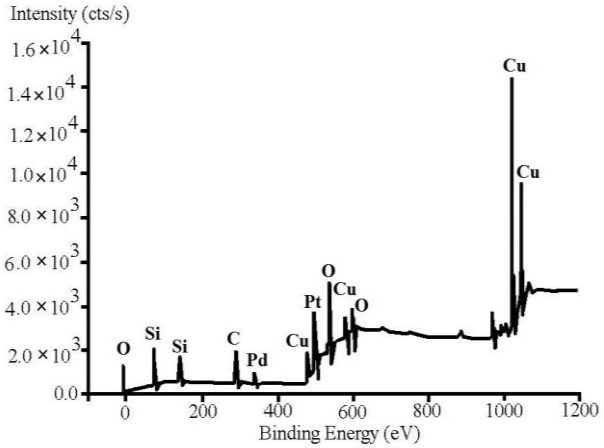

Fig. 5. Show the XPS Spectrum of 12% Pd-CuO thin films.

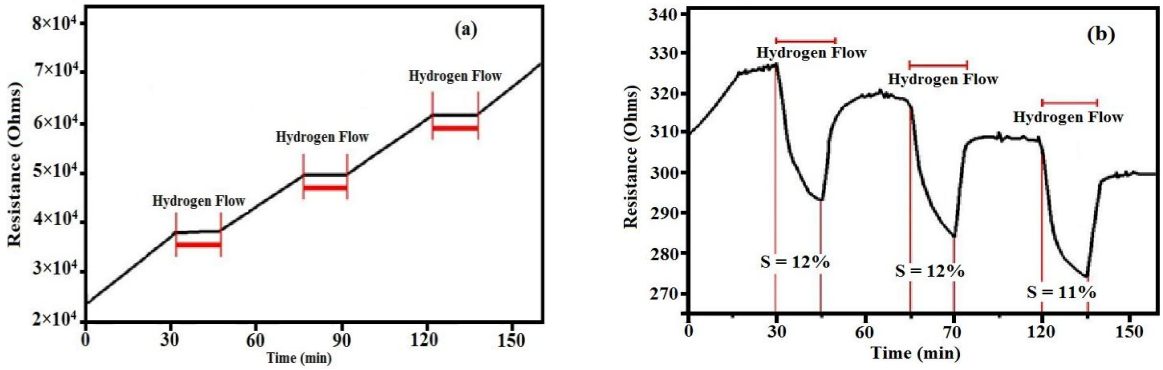

Fig. 6. Resistance results for Pd-CuO thin film with UV light exposure at room temperature.

In figure 6 (a) resistance results for 0% Pd-CuO thin film with UV light exposure at room temperature and conducted with three cycles of 100 sccm (2.5%) hydrogen gas flow and in figure 6 (b) Resistance results for 0% Pd-CuO thin film with no UV light exposure presented. Figure 7 show the previous data collected of TGS commercial sensor with UV light exposure and three cycles of 2.5% total hydrogen. The sensitivity drift rate shows a steeper drift for the commercial sensor than for the CuO thin-film sensor in Figure 8a and the baseline drift rate shows a steeper drift for the commercial sensor than for the CuO thin-film sensor in Figure 8b. Figure 9 show the Gas-sensing results of 1.0 M CuO nanoparticles with UV light exposure at room temperature with three cycles of 2.5% total hydrogen flow.

After the Pd-doped 1.0 M CuO thin-films were fabricated and annealed, grain-structure characterization of the films was done using SEM imaging. The SEM images revealed that the annealed CuO thin films were crystalline, with grains between 70 to 100 nm in diameter. The Pd-doped CuO samples showed slightly decreasing grain size with increasing dopant concentration. All of the CuO thin films showed a much

higher porosity than what was expected. In order to determine the composition of the annealed grains, EDAX was conducted using the SEM. The EDAX spectra of the CuO samples showed that the annealed thin film was made up of CuO, but, since the film was very thin, the largest peak on the spectrum is for silicon from the silicon substrate. For further demonstration, the EDAX was performed for the samples Figures 10 (a, b, c and d). The EDAX spectra of NP-CuO shown in Figure 5 manifest the presence of Cu and O as the only elementary components. This indicates that the exact concentration of the CuO thin film was not great enough to be detected by EDAX. To investigate the size distribution of the nanoparticles, a particle size histogram was prepared for CuO nanoparticles in Figure 11. Most of the particles possess sizes in the range from 70 to 90 nm.

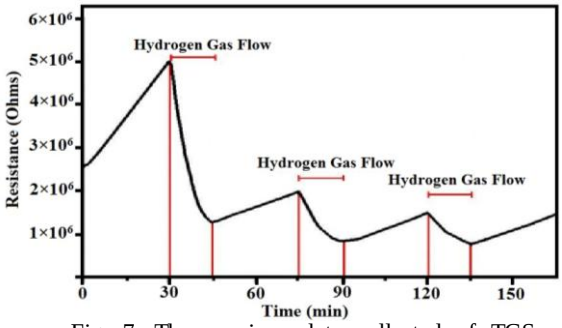

Fig. 7. The previous data collected of TGS commercial sensor.

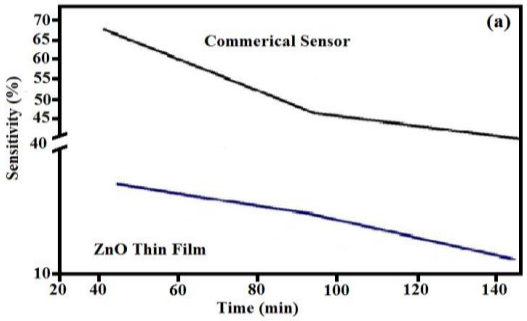

Fig. 8a

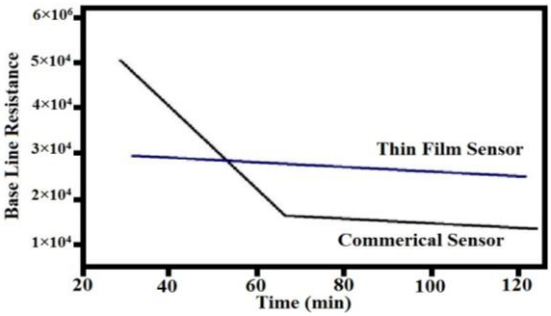

Fig. 8b. The sensitivity drift rate shows a steeper drift for the commercial sensor than for the CuO thin-film sensor.

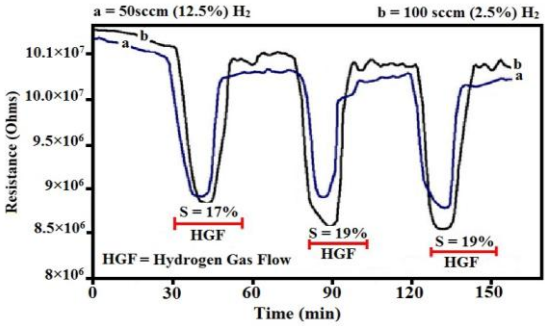

Fig. 9. Show the Gas-sensing results of CuO nanoparticles.

Gas-Sensing Characterization:

The second analysis conducted compared the pure 1.0 M CuO thin-film sensor and the TGS commercial sensor.

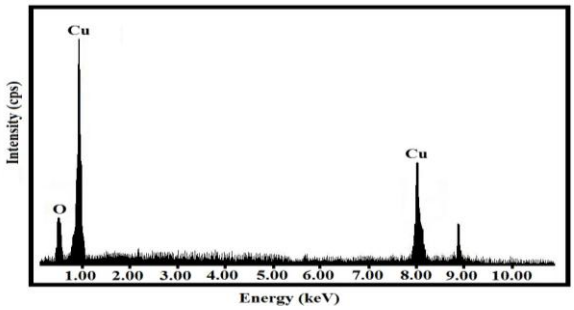

Fig. 10. The EDAX spectra of NP-CuO.

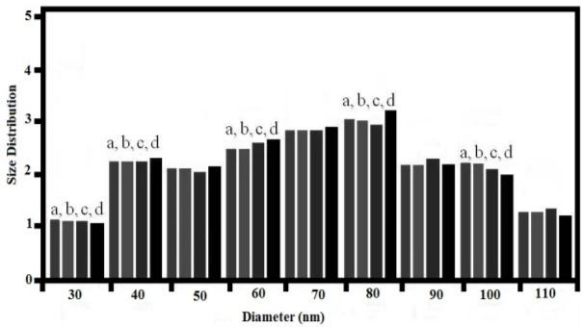

Fig. 11. Particle size histogram for CuO nanoparticles.

The measurements were taken with UV light exposure at room temperature with three cycles of 100 sccm (2.5% total) hydrogen gas flow. The analysis included a comparison in the change of sensitivity with each

exposure to hydrogen and the change in the baseline resistance with each exposure to hydrogen. These are measures of the response and recovery of the sensors; the greater the drift, the more quickly the sensor will degrade. The commercial sensor has a higher drift rate than the thin-film sensor; this is also true with the baseline drift rate. Because there was such difficulty in measuring the resistance of the Pd-doped CuO thin-film samples due to high porosity, analysis was conducted comparing the sensitivity of the CuO thin-film nanoparticle and the CuO soft-electron-beam-patterned CuO nanoparticles. The results revealed a higher sensitivity for the CuO nanoparticles (about 22%) than for the thin film (16%).

Table 1: Synthesis Parameters and size of Different CuO Nanostructures

Sample	Time (hr)	Tempreture ℃	pHi	pHf	Size
CuO-1	12	120	8	11	100 nm
CuO-2	12	150	9	11	90 nm
CuO-3	24	120	8	11	80 nm
CuO-4	24	150	9	11	70 nm

Conclusion:

Different concentrations of Pd-doped CuO sol-gels were used to fabricate nanostructures; they proved to be a simple, versatile, and inexpensive method of making sensor devices. One of the most importance observations coming from the nanoparticles characterization was that there was extremely high porosity in Pd-doped CuO nanoparticles, resulting in poor resistance measurements. EDAX and XPS confirmed the presence and concentration of Pd in the CuO thin-film samples and sol-gels, and the XRD results confirmed a crystal structure consistent with CuO for all concentrations of Pd, with no presence of second phases or shifts in d-spacing. For the gas-sensing characterization, UV light exposure increased the sensitivity of CuO in response to hydrogen, and the CuO thin film showed a better recovery than the commercial sensor at room temperature. The most important conclusion reached from the results of the gas-sensing measurements of the thin film compared with the nanoparticles is that smaller grain sizes (larger surface area), with a transition from Nano films to nanoparticles, increases the sensitivity of CuO sensor devices in response to hydrogen gas. There are several implications for the future. To continue testing on the nanostructures necessitates optimizing the annealing temperature and annealing time to refine the grain sizes and reduce the porosity of the thin films.

Acknowledgements:

Supporting of this investigation by Jundi Shapur University of Technology (Dizful, Iran) is gratefully acknowledged.

References:

[1] M.E. Franke, T.J. Koplin, U. Simon, Small 2 (2006) 36–50.

[2] G. Korotcenkov, Mater. Sci. Eng. R 61 (2008) 1–39.

[3] B.L. Cushing, V.L. Kolesnichenko, C.J. O'Connor, Chem. Rev. 104 (2004) 3893–3946.

[4] Y.W. Jun, J.S. Choi, J. Cheon, Angew. Chem. Int. Ed. 45 (2006) 3414–3439.

[5] N. Pinna, M. Niederberger, Angew. Chem. Int. Ed. 47 (2008) 5292–5304.

[6] J. Park, J. Joo, J. Kwon, S.G. Kwon, Y. Jang, T. Hyeon, Angew. Chem. Int. Ed. 46 (2007) 4630–4660.

[7] E. Comini, C. Baratto, G. Faglia, M. Ferroni, A. Vomiero, G. Sberveglieri, Progr. Mater. Sci. 54 (2009) 1–67.

[8] G. Korotcenkov, Sens. Actuators B 107 (2005) 209–232.

[9] M. Niedereberger, G. Garnweitner, N. Pinna, G. Neri, Solid State Chem. 33 (2005) 59–70.

[10] J.Q. Xu, Y.Q. Pan, Y.A. Shun, Z.-Z. TianSens. Actuators B 66 (2000) 277–279.

[11] J.J. Delaunay, N. Kakoiyama, I. Yamada, Mater. Chem. Phys. 104 (2007) 141–145.

[12] X. Jiaqiang, C. Yuping, C. Daoyong, S. Jianian, Sens. Actuators B 113 (2006) 526– 531.

[13] Y. Lv, L. Guo, H. Xu, X. Chu, Physica E 36 (2007) 102–105.

[14] C. Xiangfeng, J. Dongli, A.B. Djurisic, Y.H. LeungChem. Phys. Lett. 401 (2005) 426–429.

[15] H. Xu, X. Liu, D. Cui, M. Li, M. Jiang, Sens. Actuators B 114 (2006) 301–307.

[16] N. Yamazoe, K. Shimanoe, J. Electrochem. Soc. 155 (2008) J85–J92.

[17] M.HyunSeo, M. Yuasa, T. Kida, J. Soo Huh, K. Shimanoe, N. Yamazoe, Sens. Actuators B 137 (2009) 513–520.

[18] Li, Y.; Meng, G. W.; Zhang, L. D. Appl. Phys. Lett. 2000, 76, 2011.

[19] Zheng, M. J.; Zhang, L. D.; Li, G. H.; Shen, W. Z. Chem. Phys. Lett. 2002, 363, 123.

[20] Lee, W.; Jeong, M.-C.; Myoung, J.-M. Nanotechnology 2004, 15, 1441.

[21] K.W. Commander, A. Prosperetti, J. Acoust. Soc. Am. 85 (1988) 732.

[22] S. Da¨hnke, F.J. Keil, Ind. Eng. Chem. Res. 37 (1998) 848.

[23] S. Iijima, Nature 354 (1991) 56.

[24] M.Y. Yen, C.W. Chiu, C.H. Hsia, F.R. Chen, J.J. Kai, C.Y. Lee, H.T. Chiu, Adv. Mater. 15 (2003) 235.

[25] J.B. Chang, J.Z. Liu, P.X. Yan, L.F. Bai, Z.J. Yan, X.M. Yuan, Q. Yang, Mater. Lett. 60 (2006) 2125.

[26] Z. Liu, Y. Bando, Adv. Mater. 15 (2003) 303.

[27] Wang et al. Appl. Phys. Lett. 2004, 84, 18, 3654–3656.

[28] Wang et al. Appl. Phys. Lett. 2005, 86, 243503–(1–3).

[29] Mitra, P; Chatterjee, A. P. Maiti, H. S. Materials Letters 1996, 35, 33–38.

[30] Tien et al. Appl. Phys. Lett. 2005, 87, 222106–(1–3).

[31] Franke, M. E.; Koplin, T. J.; Simon, U. Small 2006, 2:1, 36–50.

[32] Yamazoe, N.; Shimanoe, K.; Sawada, C. Thin Solid Films 2007, 515, 8302–8309.

[33] Donthu, S.; Sun, T.; Dravid, V. Adv. Mater. 2007, 19, 125–128.

[34] Alireza Aslani, A. R. Bazmandegan-Shamili and Shahram Barzegar, Physica B, 405 (2010) 3585–3589.

[35] Alireza Aslani, A. R. Bazmandegan-Shamili and Karim Kaviani, Physica B, 405 (2010) 3972–3976.

[36] R. R. Karimi, A. R. B. Shamili, Alireza Aslani and Karim Kaviani, Physica B, 405 (2010) 3096–3100.

[37] Alireza Aslani, Physica B, 406 (2011) 150–154.

[38] Alireza Aslani and Vahid Oroojpour. Physica B, 406 (2011) 144–149.